UDC 539.4

Cyclic Inelasticity and High-Cycle Fatigue of Metals with Consideration of the Stress Gradient Effect*

V. T. Troshchenko

Pisarenko Institute of Problems of Strength, National Academy of Sciences of Ukraine, Kiev, Ukraine

vtt@ipp.kiev.ua

УДК 539.4

Циклическая неупругость и многоцикловая усталость металлов с учетом эффекта градиента напряжений

В. Т. Трощенко

Институт проблем прочности им. Г. С. Писаренко НАН Украины, Киев, Украина

Исследуется циклическое деформирование металлов и сплавов при многоцикловом циклическом нагружении в условиях неоднородного напряженного состояния. Показано существенное влияние градиента напряжений на циклическую неупругую деформацию поверхностных слоев металла. Обоснована модель, позволяющая объяснить различие между пределами выносливости при однородном и неоднородном напряженных состояниях по диаграммам циклического нагружения. Модель учитывает то, что предел выносливости равен пределу циклической упругости при уровне неупругой деформации, характерном для конкретного класса материала.

Ключевые слова: многоцикловая усталость, циклическая неупругость, градиент напряжений.

Introduction. It is well known that the fatigue strength of metals and alloys in the nonuniform stressed state (bending, torsion of solid specimens, local stresses in the stress concentrator) is much higher than that in the uniform stressed state.

Different approaches are used to explain the nonuniform stressed state effect, which is usually characterized by the value of the stress gradient.

It is assumed in some studies that the difference between the fatigue limits in the uniform and nonuniform stressed states is explained by distinctions between the real stresses, which are calculated accounting for cyclic inelasticity (cyclic plasticity), and nominal stresses determined from the formulas of the elasticity theory [1].

In other investigations, the difference between the fatigue limits in the uniform and nonuniform stressed states is explained on the basis of fractal approach [2, 3] or statistical strength theories, primarily those based on the "weak link" concept [4, 5].

* Report on International Colloquium "Mechanical Fatigue of Metals" (13–15 September 2010, Opole, Poland).

In recent years, a concept of the "critical distance" has been developed, which is based on the assumption that fatigue fracture is caused either by the stresses at some distance from the surface or by average stresses in the surface layer of a certain thickness [6].

At the same time, as was found in many experimental investigations, account should be taken of the fact that the process and characteristics of high-cycle inelastic deformation of the surface layers of nonuniformly stressed specimens differ significantly from those of the uniformly stressed ones.

This paper summarizes the results of published and original investigations of the cyclic deformation behavior of metals and alloys in the nonuniform and uniform stressed states, and a model is proposed, which allows explaining the difference between the fatigue limits of metals and alloys under such loading conditions.

1. **Fatigue and Inelasticity of Metals under Uniform Axial Loading**. The stage of nonlocalized fatigue damage leading to the initiation of the main fatigue crack is characterized by the formation and growth of local microplastic deformation zones where microcracks initiate and one of them develops into the main fatigue crack that leads to final fracture [7].

As shown in [8], the number of cycles to the initiation of a 0.05 mm fatigue crack in smooth metallic specimens makes up 90% and more of their total life.

The integral characteristics of the processes of local microplastic deformation are the inelastic strain per cycle $\Delta\varepsilon_i$ equal to the width of a hysteresis loop in the stress amplitude σ_a – strain amplitude ε_a coordinates and the inelastic strain energy ΔW equal to the hysteresis loop area in these coordinates.

For high-cycle fatigue of most structural alloys at stresses corresponding to 10^7 and more cycles to fracture, the $\Delta\varepsilon_i$ and ΔW values are rather small and difficult to study; nevertheless, they are the characteristics defining the process of the fatigue crack initiation.

Figures 1a and 1b illustrate the stress and strain variation under elastic and inelastic deformation, respectively; Fig. 1c shows schematic dependences of inelastic strain per cycle on the number of the load cycles at $\sigma_a = \text{const}$ for cyclically softening (*1*), cyclically stable (*2*), and cyclically hardening (*3*) materials. Figure 1d presents static (*I*) and cyclic (*II*) stress–strain diagrams for the load cycle numbers N_1 and N_2.

The strain amplitude can be calculated as the sum of the elastic $\Delta\sigma/2E$ and inelastic $\Delta\varepsilon_i/2$ strains:

$$\varepsilon_a = \frac{\Delta\sigma}{2E} + \frac{\Delta\varepsilon_i}{2}.$$

According to the Ramberg–Osgood equation

$$\varepsilon_a = \frac{\Delta\sigma}{2E} + \left(\frac{\Delta\sigma}{2K'}\right)^{n'},$$

where n' and K' are material constants.

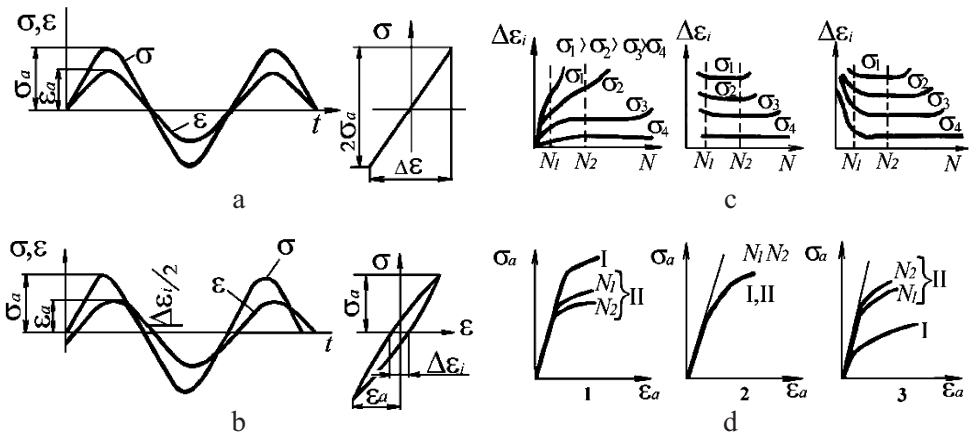

Fig. 1. Stresses and strains under high-cycle loading.

The cyclic elasticity limit σ_e^c equal to stresses at a certain tolerance for residual strain (offset strain value) was determined from the cyclic stress–strain diagram. In our case, residual strain corresponds to the inelastic strain amplitude. With an offset strain value of, for instance, $1\cdot10^{-5}$ mm/mm, or $1\cdot10^{-3}$ in percent, the cyclic elasticity limit is denoted by $\sigma_{0.001}^c$, etc.

Investigations of cyclic inelastic strains of metals and alloys were performed using the procedures described in [9].

The inelastic strain per cycle was directly measured as a strain value corresponding to zero stress in the process of symmetric cyclic loading (Fig. 1b). To perform those investigations special equipment was designed that allowed high-frequency scanning of the stress and strain signals and processing of the measurement results on a computer in real time [9]. In some cases, inelastic strain per cycle was measured from the hysteresis loop on the oscilloscope screen. The loading frequency varied from 20 to 36 Hz.

The results of investigations are summarized in Table 1, where σ_u is the ultimate strength, $\sigma_{0.2}$ is 0.2% offset yield stress, σ_{-1} is fatigue limit for 10^7 cycles, $(\Delta\varepsilon_i)_{\sigma_{-1}}$ is the inelastic strain amplitude corresponding to the fatigue limit, and $(\Delta\varepsilon_i)_{\max}$ is the maximum inelastic strain amplitude observed for the material studied [6].

The values $(\Delta\varepsilon_i)_{\sigma_{-1}}$ and $(\Delta\varepsilon_i)_{\max}$ were determined from inelastic strain measurements at its stabilization stage or at a half of loading cycles to fracture.

To increase the accuracy of determining $(\Delta\varepsilon_i)_{\sigma_{-1}}$, the results of testing several specimens at different stresses in the "$\sigma_a - \lg\Delta\varepsilon_i$" coordinates were processed by the least squares method, $(\Delta\varepsilon_i)_{\sigma_{-1}}$ was determined as the abscissa of the intersection point of the approximated line and the horizontal line corresponding to the fatigue limit.

The main results presented in Table 1 were obtained at room temperature; some materials were tested at low and high temperatures as is shown in Table 1.

T a b l e 1

Fatigue Limits and Characteristics of Cyclic Inelasticity of Metals and Alloys

Material	σ_u, MPa	$\sigma_{0.2}$, MPa	σ_{-1}, MPa	$\left(\frac{\Delta\varepsilon_i}{2}\right)_{\sigma_{-1}} \cdot 10^5$	$\left(\frac{\Delta\varepsilon_i}{2}\right)_{\max} \cdot 10^5$
1	2	3	4	5	6
Carbon steels					
Steel 25 (0.25% C)	518	–	167	1.50	80.0
Steel 30 (0.30% C)	726	414	340	0.83	14.0
Steel 45(I) (0.45% C)	668	408	230	6.70	190.0
Steel 45(II) (0.45% C)	716	468	270	9.30	130.0
Steel 60 (0.60% C)	937	622	177	2.60	22.0
Alloyed steels					
Steel 20Kh (0.20% C, 0.85% Cr)	500	–	157	1.30	40.0
Steel 40Kh(I) (0.40% C, 0.95% Cr)	994	899	360	1.80	28.0
Steel 40Kh(II) (0.40% C, 0.95% Cr)	873	590	300	3.30	45.0
Steel 40Kh(III) (0.40% C, 0.95% Cr)	840	675	330	0.02	90.0
Steel 1Kh13(I) (0.12% C, 13.0% Cr)	638	429	283	0.23	14.0
Steel 1Kh13(I) (773 K) (0.12% C, 13.0% Cr)	–	–	140	2.30	115.0
Steel 1Kh13(II) (0.12% C, 13.0% Cr)	620	390	270	2.00	15.0
Steel 1Kh13(III) (0.12% C, 13.0% Cr)	746	614	350	0.40	15.0
Steel 12KhN3 ($C \le 0.17\%$, 0.95% Cr)	624	17	270	0.38	100.0
Steel 09Kh14N19V2BR1 (0.1% C, 14% Cr, 35.0% Ni)	560	–	147	1.10	50.0
Steel 1Kh17N2Sh (0.1% C, 14.0% Cr, 35% Ni)	912	707	390	1.60	21.0
Steel KhN35VT(I) (0.1% C, 15.0% Cr, 35.0% Ni)	1000	595	300	0.45	41.0
Steel KhN35VT(I) (873 K) (0.1% C, 15.0% Cr, 35.0% Ni)	850	450	290	2.10	28.0
Steel 15KhN35VT(II) (0.1% C, 15.0% Cr, 35.0% Ni)	896	582	260	0.15	9.0
High-ductility austenitic and other steels					
Steel 1Kh18N10T (0.12% C, 18.0% cr, 10.0% Ni)	650	250	190	16.80	100.0
Steel 30Kh10G10 (0.28% C, 11.0% Cr, 10.5% Mn)	815	397	320	11.60	103.0
Steel 0Kh14AG12M	1018	435	310	14.30	125.0
Steel 15G2AFDps(I) (0.16% C, 1.46% Mn)	520	420	260	14.00	14.0
Steel 15G2AFDps(II) (0.16% C, 1.46% Mn)	532	410	250	11.50	11.5

Continued Table 1

1	2	3	4	5	6
Nickel alloys					
Alloy KhN77TYuR (C ≤ 0.07%, 20.0% Cr, 2.7% Ti)	1240	670	360	–	22.3
Alloy KhN77TYuR (933 K) (C ≤ 0.07%, 20.0% Cr, 2.7% Ti)	980	480	360	1.40	26.0
Alloy KhN70VMTYuF (C ≤ 0.12%, 20.0% Cr, 6.0% W)	960	650	620	0.03	11.0
Alloy KhN70VMTYuF (1153 K) (C ≤ 0.12%, 20.0% Cr, 6.0% W)	610	570	210	0.17	17.0
Aluminum-based alloys					
Alloy D16T (4.3% Cu, 0.6% Mn)	538	398	120	2.40	13.0
Alloy D20 (6.5% Cu, 0.6% Mn)	410	250	60	2.50	11.0
Alloy D20 (77 K) (6.5% Cu, 0.6% Mn)	523	340	80	1.20	17.0
Copper and copper-based alloys					
Copper (annealed)	232	70	100	0.43	48.0
Brass L62 (62.0% Cu, 38.0% Cu)	449	371	150	0.78	146.0
Bronze Br AZh9 (81.4% Cu, 3.74% Ni)	688	315	260	0.59	80.0
Cast iron					
Cast iron SCh 21-40	225	–	100	2.80	6.0

Some of the investigated materials were subjected to various thermal treatments and test specimens were fabricated from different batches of the material that is indicated by indices I, II, and III.

Table 1 also gives the content of carbon and some alloying elements for the steels and alloys investigated.

The results presented in Table 1 demonstrate that, in the region of high-cycle fatigue, cyclic inelastic strains are considerably lower than cyclic plastic strains under low-cycle loading; their investigation is widely covered in the literature. Moreover, Table 1 shows that for different metals and alloys the inelastic strain amplitude $(\Delta\varepsilon_i/2)_{\sigma_{-1}}$ corresponding to the fatigue limit varies within a wide range.

Despite such a broad range of inelastic strain values corresponding to the fatigue limits of different metals and alloys tested during 10^7 cycles, by classifying all metals and alloys in groups, one can derive a rather exact relationship between the fatigue limits and elasticity limits obtained from cyclic stress–strain diagrams with certain tolerances for inelastic strain [9].

Figure 2a compares the fatigue limits σ_{-1} and cyclic elasticity limits σ_e^c for carbon, alloyed and austenitic steels, copper and copper-based alloys when the cyclic fatigue limit for all these materials is determined with a common offset strain value $\Delta\varepsilon_i/2$ equal to $1\cdot10^{-5}$. In this case, a wide scatter of results is observed.

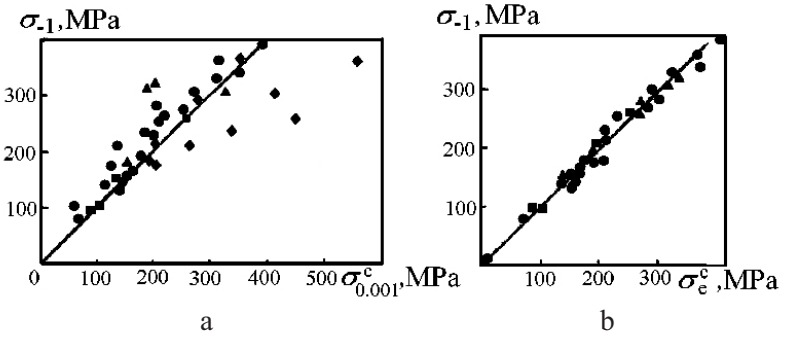

Fig. 2. Comparison of the fatigue limits and cyclic elasticity limits of materials of different classes with common (a) and differentiated (b) offset strain values: (●) carbon and alloy steels; (▲) austenitic steel; (◆) copper-based alloys.

If we take $\sigma_{-1} = \sigma^c_{0.002}$ for carbon and alloyed steels, $\sigma_{-1} = \sigma^c_{0.015}$ for ductile austenitic steels, and $\sigma_{-1} = \sigma^c_{0.0005}$ for copper and copper-based alloys, the discrepancies in determining the fatigue limits for corresponding metals and alloys from the values of cyclic elasticity limits will not exceed $\pm 10\%$ (Fig. 2b).

The analysis performed in [10] revealed that with the inelastic strains characteristic of most metals and alloys at stresses equal to the fatigue limit for a test duration of 10^7 cycles to failure, the difference between real and nominal stresses is insignificant and cannot account for the distinction between the fatigue limits in the uniform and nonuniform stressed states.

2. **Cyclic Deformation Behavior of Metals and Alloys in the Nonuniform Stressed State**. Studies on the inelastic cyclic deformation behavior of metals and alloys under high-cycle loading in the nonuniform stressed state, especially at stresses close to the fatigue limit, are limited in number.

From analysis of the inelastic deformation behavior and fatigue failure of metals in the nonuniform stressed state the following can be noted.

At the same level of stresses, microplastic strains develop less intensively in the surface layers of a nonuniformly stressed specimen than in the uniformly stressed one.

In accordance with [11], Fig. 3 presents, the relation between ω_k, which is the ratio of the number of plastically deformed local volumes (grains) on the specimen surface at the deformation stabilization stage to the total number of grains, and the stress amplitude σ_a for low-carbon steel ($\sigma_u = 421$ MPa and $\sigma_{0.2} = 267$ MPa) (Fig. 1a) and copper ($\sigma_u = 268$ MPa and $\sigma_{0.2} = 190$ MPa) (Fig. 1b) under symmetrical high-cycle loading. In this figure, curve *1* corresponds to axial loading, curves *2* and *3* – to bending with 0.2 and 2.0 mm^{-1} relative stress gradients, respectively.

The relative stress gradient in bending within the maximum stress zone equals to $\overline{\eta} = \dfrac{1}{\sigma_{\max}} \dfrac{d\sigma}{dx}_{x=0}$. Solid symbols on the curves correspond to the fatigue limit values.

As follows from the data of Fig. 3, the process of cyclic inelastic deformation of the metal surface layer is greatly dependent on the stress gradient.

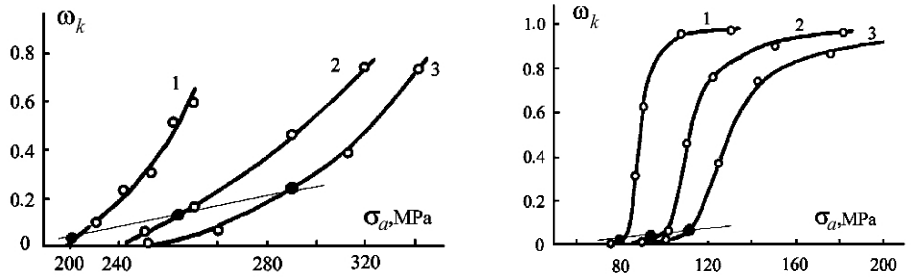

Fig. 3. ω_k vs σ_a relations under axial loading and in bending: (a) low-carbon steel, (b) copper.

With an increase in the stress gradient, the stress value, at which an equal degree of surface damage ($\omega_k = \text{const}$) is achieved, increases.

Similar nature of deformation behavior of the material surface layers in the uniform and nonuniform stressed states was also observed in [12, 13, and others].

Strain amplitudes corresponding to the initiation of a fatigue crack of a certain size at a given number of loading cycles in the nonuniform stressed state (bending, stress concentrators), are much higher than those under axial loading [14–17 and others]. This difference becomes more significant with an increase in the number of cycles to crack initiation. Figures 4 and 5a illustrate the results obtained experimentally in [16, 17].

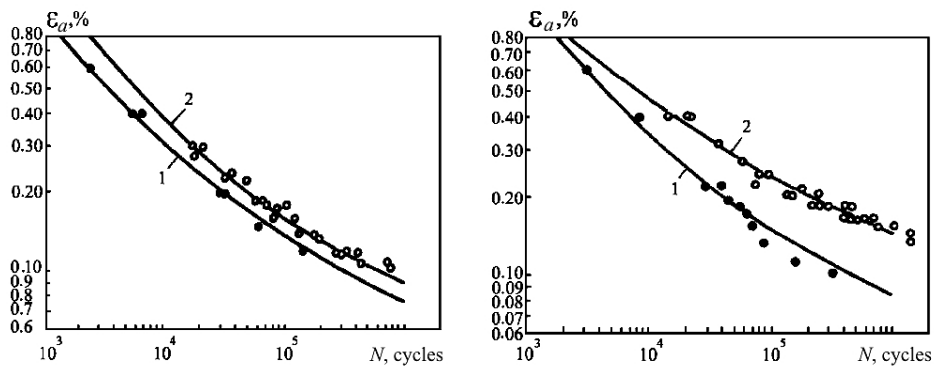

Fig. 4. ε_a vs N relations under symmetrical tension for coarse-grained (a) and fine-grained (b) steels: (*1*) smooth specimens, (*2*) specimens with stress concentrators $K_t = 1.54$ and 2.57).

The values of inelastic strains per cycle, which correspond to the initiation of fatigue cracks at the same number of loading cycles in the uniform and nonuniform stressed states, are either independent of the loading type [17] (Fig. 5b) or somewhat higher in the nonuniform stressed state than in the uniform one [11, 18].

From the results presented here it follows that the experimental cyclic stress–strain diagrams in bending within the region of stresses corresponding to high-cycle fatigue in the "nominal stress ($\sigma_a^{nom} = M_{bend}/W$) – strain amplitude" coordinates differ from similar diagrams calculated with the use of the cyclic stress–strain diagrams under axial loading [19].

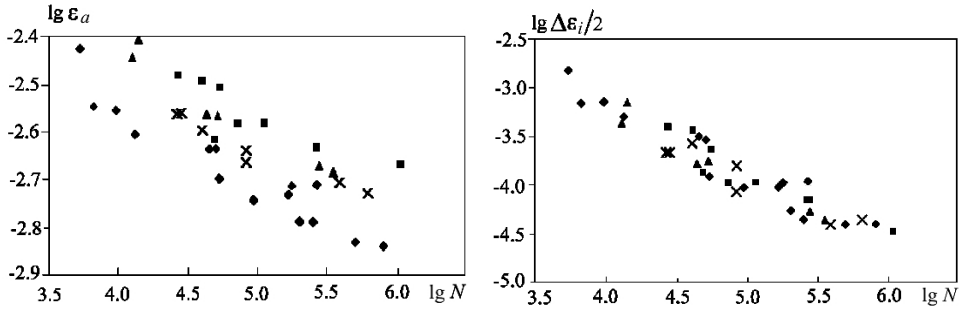

Fig. 5. $\lg\varepsilon_a$ vs $\lg N$ (a) and $\lg\Delta\varepsilon_i/2$ vs $\lg N$ (b) relations for steel 30KhGSA: (◆) smooth specimens, (■, ▲, ×) specimens with theoretical stress concentration factors K_t = Kt = 2.27, 2.06, and 1.23.

3. **Summary of Results**. With the account of the above results, the fatigue limit vs stress gradient relationships can be explained using the model based on the following basic assumptions.

Cyclic stress–strain diagram for the material most stressed surface layers depends on the stress gradient and is described by the following relations:

$$\varepsilon_a = \frac{\sigma_a}{E} + \left(\frac{\sigma_a - \sigma^c_{pr}(\overline{\eta})}{K}\right)^n \qquad \text{at} \qquad \sigma_a > \sigma^c_{pr}(\overline{\eta}),$$

$$\varepsilon_a = \frac{\sigma_a}{E} \qquad \text{at} \qquad \sigma_a < \sigma^c_{pr}(\overline{\eta}),$$

where $\sigma^c_{pr}(\overline{\eta})$ is the cyclic proportionality limit at the stress gradient $\overline{\eta}$ (this function can be found from summarized experimental results), and K and n are material constants.

The fatigue limit at a given stress gradient is equal to the cyclic elasticity limit obtained from the corresponding cyclic stress–strain diagram with the offset strain value typical of a given class of material. This offset strain value equals to the inelastic strain amplitude per cycle corresponding to the number of cycles to fracture at which the fatigue limit is determined.

Figure 6 shows schematically cyclic stress–strain diagrams for the material at different relative stress gradients $\overline{\eta}$ and fatigue limits $\sigma_{-1}(\overline{\eta})$, corresponding to these stress gradients, on the assumption that the offset strain value, which corresponds to the fatigue limit, equals to $\Delta\varepsilon_i/2$.

The results obtained, e.g., in [18] demonstrating that inelastic strains, corresponding to the fatigue limit, increase with the stress gradient, can be described within the model presented on the assumption that the offset strain value in determining the cyclic elasticity limit, corresponding to the desired fatigue limit, increases with the stress gradient (line AC in Fig. 6).

The scheme in Fig. 6 can be used for describing the above cyclic deformation behavior of metals in the nonuniform stressed state (Figs. 3–5).

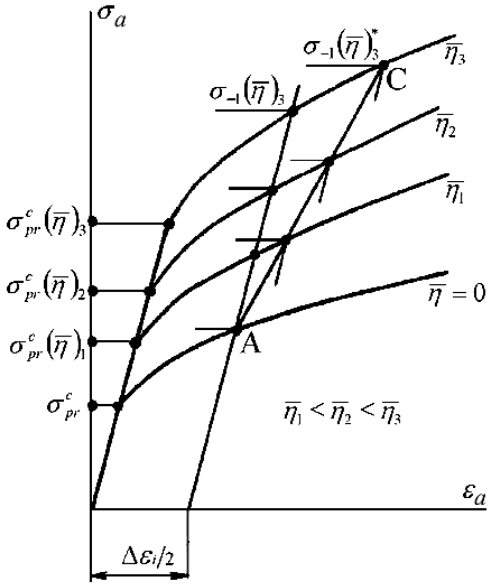

Fig. 6. Cyclic stress–strain diagrams for metals taking into account the stress gradient effect.

As also follows from the scheme, the nominal stress–strain diagram in bending in the "nominal stress amplitude – strain amplitude of the specimen surface layer ε_a" coordinates should be calculated using the diagrams given in Fig. 6 rather than the stress–strain diagram under axial loading.

In this case, the difference between the real and nominal stresses in bending will take place only at stresses above $\sigma^c_{pr}(\overline{\eta})$. This should be taken into account when considering the stressed state in stress concentrators.

The difference between the cyclic proportionality limits under axial loading ($\overline{\eta} = 0$) and in bending ($\overline{\eta} = 0.13$ mm^{-1}) for carbon, low-alloyed, and austenitic steels and copper were studied in [19]. Results of those investigations are presented in Fig. 7, which shows variation of the ratio between the cyclic proportionality limits under bending and axial loading, K_η, and the ratio between the cyclic proportionality limits under axial loading and those under static loading, K_c, depending on the ratio between the static proportionality limit and the ultimate strength σ_{pr}/σ_u.

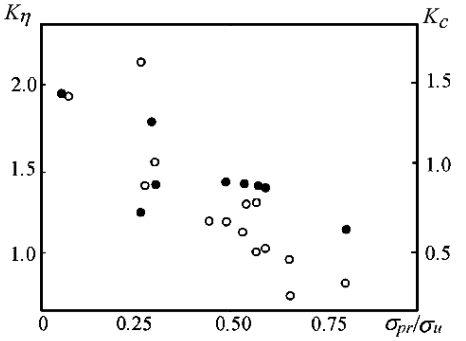

Fig. 7. Variation of K_η (●) and K_c (○) values depending on the σ_{pr}/σ_u ratio.

Despite a large scatter of results, a conclusion can be made that the ratio K_η decreases with increasing σ_{pr}/σ_u and that the K_η and K_c values behavior is similar.

Such investigations aimed at studying peculiarities of cyclic hardening and softening of metals in the region of small cyclic inelastic strains with allowance for the influence of the stress gradient call for further development.

Conclusions. The difference in the inelastic cyclic deformation behavior of the most stressed surface layers of metals and alloys in the uniform and nonuniform stressed states under high-cycle loading has been considered.

Analysis of all the above results shows that real cyclic stress–strain diagrams for metals and alloys in the inelastic region depend on stress gradients and shift towards the region of higher stresses with an increase in the stress gradients.

An equation for the cyclic stress–strain diagram, which considers the stress gradient effect, is proposed and substantiated, and an explanation is given for the dependence of the fatigue limit on the stress gradient, which is based on accounting for the dependence of cyclic stress–strain diagrams on the stress gradient and on the correlation between the fatigue limits and cyclic elasticity limits obtained with offset strain values typical of the material studied.

Р е з ю м е

Досліджується циклічне деформування металів і сплавів за багатоциклового циклічного навантаження в умовах неоднорідного напруженого стану. Показано суттєвий вплив градієнта напружень на циклічну непружну деформацію поверхневих шарів металу. Обґрунтовано модель, яка дозволяє пояснити відмінність між границями витривалості за однорідного і неоднорідного стану згідно з діаграмами циклічного навантаження. Модель враховує те, що границя витривалості дорівнює границі циклічної пружності при рівні непружної деформації, характерному для конкретного класу матеріалів.

1. I. Oding, *Allowable Stresses in Machine Building and Cyclic Strength of Metals* [in Russian], Mashgiz, Moscow (1962).
2. A. Carpinteri, A. Spagnoli, and S. Vantadori, “An approach to size effect in fatigue of metals using fractal theories,” *Fatigue Fract. Eng. Mater. Struct.*, **25**, 619–627 (2002).
3. A. Carpinteri, A. Spagnoli, and S. Vantadori, “Size effect in *S–N* curves: a fractal approach to finite-life fatigue strength,” *Int. J. Fatigue*, **31**, 927–933 (2009).
4. W. Weibull, *A Statistical Theory for the Strength of Materials*, Swedish Royal Institute for Engineering Research, Stockholm (1939).
5. T. Delahay and T. Palin-Luc, “Estimation of the fatigue distribution in high-cycle multiaxial fatigue taking into account the stress-strain gradient effect,” *Int. J. Fatigue*, **28**, 474–484 (2006).
6. D. Taylor, *The Theory of Critical Distances: A New Perspective in Fracture Mechanics*, Elsevier, Oxford (2006).

7. V. T. Troshchenko, “Nonlocalized fatigue damage of metals and alloys. Part 1. Inelasticity, investigation methods, and results,” *Strength Mater.*, **37**, No. 4, 337–356 (2005).
8. S. Manson, “Fatigue: A complex subject – some simple approximations,” *Exp. Mech*., **5**, 193–226 (1965).
9. V. T. Troshchenko, L. A. Khamaza, G. V. Tsybanev, *Methods for Accelerated Determination of Endurance Limits of Metals Based on Strain and Energy Criteria* [in Russian], Naukova Dumka, Kiev (1979).
10. V. T. Troshchenko and L. A. Khamaza, “Influence of inelastic strains on the fatigue limit of metais during bending,” *Strength Mater.*, **8**, No. 4, 387–392 (1976).
11. R. Holzman, “Vliv nehomogenni napjatosti na mezni stav pri cyklickem zatezavani,” *Strojnicky Casopis*, **5**, 419–442 (1964).
12. S. Taira, “X-ray approach to the study on mechanical behavior of metals,” in: Proc. Int. Conf. on *Mechanical Behavior of Materials* (Kyoto, Japan) (1971).
13. J. He, H. Wang, and J. Nan, “Fatigue strength evaluation from surface yielding data,” *Fatigue Fract. Eng. Mater. Struct.*, **16**, 591–596 (1993).
14. K. Iida, “Comparison of fatigue strength of steel under deflection-controlled bending and strain-controlled axial load cycling,” in: Proc. Second Int. Conf. on *Mechanical Behavior of Materials* (Boston) (1976), pp. 759–764.
15. S. Kotani, K. Koibuchi, and K. Kasai, “The effect of notches on cyclic stress–strain behavior and fatigue crack initiation,” in: Proc. Second Int. Conf. on *Mechanical Behavior of Materials* (Boston) (1976), pp. 606–610.
16. S. Lane and H. Bomas, “Spectrum fatigue assessment of notched specimens based on the initiation and propagation of short cracks,” *Int. J. Fatigue*, **28**, 1011–1021 (2006).
17. P. Fomichev, “Life assessment parameter for bodies with stress concentrators,” in: Proc. Int. Conf. on *In-Service Damage of Materials. Diagnostics and Prediction Methods* (Ternopol) (2009), pp. 82–89.
18. G. Horwood and D. White, “Strain localization in beams under cyclic plastic straining at room and elevated temperature,” *J. Strain Analysis*, **6**, 108–120 (1971).
19. V. T. Troshchenko, *Fatigue and Inelasticity of Metals* [in Russian], Naukova Dumka, Kiev (1971).

Received 04. 04. 2011